Available online at www.sciencedirect.com
SCIENCE DIRECT
Polymer 47 (2006) 1689–1695
polymer
www.elsevier.com/locate/polymer

Investigation of the crystallization of m(LLDPE) under shear flow using rheo-optical techniques

F. Chaari [a], M. Chaouche [a,*], L. Benyahia [b], J.F. Tassin [b]

[a] LMT Cachan/CNRS/Univeristé, Paris 6. 61 Avenue du Président Wilson, 94235 Cachan, Cedex, France
[b] Laboratoire Polymères, Colloïdes, Interfaces, Université du Maine. Avenue Olivier Messiaen, 72085 Le Mans, Cedex, France

Received 4 June 2004; received in revised form 11 July 2005; accepted 4 January 2006
Available online 27 January 2006

Abstract

Metallocene linear low density polyethylene (mLLDPE) crystallization under shear flow at different controlled shear rates was investigated experimentally between its quiescent crystallization temperature and its melting point temperature (T_m). The evolution of the material optical properties, including turbidity, birefringence and dichroism, was monitored following a temperature jump from a temperature much higher than T_m to a fixed crystallization temperature (T_c). These properties are discussed in terms of the evolution of the polymer semi-crystalline microstructure. In light of the optical properties evolution, the crystallization process can be split into three stages (i) incubation phase in which small (compared to the light wavelength) crystalline nuclei spread over the medium, (ii) isotropic crystallite growth phase and (iii) anisotropic crystallite growth phase. The optical properties evolution due the development of the crystallization is compared to that of the stress under the same thermo-mechanical conditions. It is observed that the optical properties are more sensitive than the stress to follow the crystalline development, in particular during the early stage of the process.

Keywords: Flow-induced crystallization; Rheo-optics; mLLDPE

1. Introduction

A number of thermoplastic polymers, in particular those presenting stereoregularity, can partially crystallize between their glass transition temperature (T_g) and their melting temperature. It is well known that straining such polymers in this temperature range enhances the crystallization rate and gives rise to anisotropic and complex semi-crystalline microstructures. The crystallization process affects considerably the rheological properties of the polymer. This can be then used as an experimental tool to follow the crystalline development under strain. In order to characterize the semi-crystalline texture development one has to include a local physical measurement. The use of different measurement techniques, including X-ray diffraction, infrared spectroscopy, etc. has been reported in the literature [1–4]. In most of these experiments, the physical measurements were performed ex situ, after the completion of the deformation and the quenching of the polymer. In such experimental procedure one assumes that the relaxation effects and thermal crystallization during quenching can be ignored. However, a number of recent experiments showed that unexpected phenomena can be encountered when undertaking on-line measurements. For instance Blundell et al. [5] reported a series of experiments in which poly(ethylene terephthalate) films were drawn slightly above T_g, and simultaneously, synchrotron X-ray diffraction patterns at rates as high as a pattern per 40 ms were recorded. They reported the intriguing phenomenon that (at high draw rates) the deformation inhibited the crystallization development, and the later was delayed until the end of the deformation. Chaari et al. [6] reported similar Synchrotron experiments in which they found that crystallization can either start during the deformation and continues during stress relaxation, or takes place wholly during the deformation, depending upon the deformation rate.

A polymer undergoing both deformation and crystallization is characterized by an anisotropic microstructure; it will then anisotropically transmit or absorb a polarised light. In the present study, both birefringence (anisotropic transmission) and dichroism (anisotropic attenuation) of light passing through a sample of mLLDPE undergoing shear flow and crystallization are used to characterize the material's

* Corresponding author. Tel.: +33 1 47 40 22 47; fax: +33 1 47 40 22 40.
E-mail address: chaouche@lmt.ens-cachan.fr (M. Chaouche).

0032-3861/$ - see front matter © 2006 Elsevier Ltd. All rights reserved.
doi:10.1016/j.polymer.2006.01.017

semi-crystalline microstructure. A similar rheo-optical study of shear-induced crystallization has been recently reported in the literature [7]. However, the polymer system considered (poly(ε-caprolactone)) led to an optical behaviour qualitatively different from ours, as discussed in Section 3. Actually, most of rheo-optical studies of strain-induced crystallization reported in the literature deal with extensional flow geometries [8–10] or polymer drawing at temperature close to T_g [11,12]. On the other hand, under shear flow and low supercooling conditions, the strain-induced orientation of molecular segments is in general less significant, which would lead to small flow-induced birefringence signals, in particular at the early stage of the crystallisation process. For this reason, the polymer chosen in this study is characterized by its high molecular weight, subsequently a long molecular average relaxation time. Moreover, it has a narrow molecular weight distribution since it is metallocene-catalyzed. Recently, Chai et al. [13] considered the influence of pre-shearing on the crystallization of mLLDPE compared to that of a conventional (Ziegler–Natta catalyzed), at relatively high temperatures (>150 °C). This investigation was undertaken using rheological measurements combined with small angle light scattering. However, they found no significant influence of the shear on the crystallization of mLLDPE under the thermo-mechanical conditions they considered.

The purpose of the present study is to consider the crystallization of mLLDPE under shear flow through the anisotropic optical properties of the induced microstructure (both in amorphous and crystalline phases). In order to achieve valuable polarimetry signals, the experiments were performed under conditions of relatively high degree of supercooling ($T_m - T_c$), although the working temperature remained above that of the quiescent crystallization of the material. Finally, effective viscosity measurements were undertaken under the same thermo-mechanical conditions. Then, the efficiency of the rheological method to follow the crystallization process is compared to that of the optical one.

2. Experiments

The metallocene linear low density polyethylene (EXCEED™ 1327 A) used for this study was kindly supplied by EXXON. Its average molecular weight was 110 kg mol^{-1}. The thermal properties of the polymer were investigated using DSC measurements. The melting temperature was found to be about 129 °C, and the maximum thermal crystallization upon cooling occurred around 107 °C. Because of its high viscosity at the working temperature, and in order to avoid bubble formation in the sample during its loading in the shear cell, the polymer was mould-injected into 1.2 mm thick discs. The optical experiments were carried out using a LINKAM CSS450 shear cell. The samples were sheared between two parallel quartz plates, with a fixed gap of 1 mm. During all the experiments, the temperature was controlled to within 0.1 °C by heating both the two plates. The rotation speed of the lower disc was adjusted to obtain the desired shear rate at the observation point (located at 7.5 mm from the rotation axis).

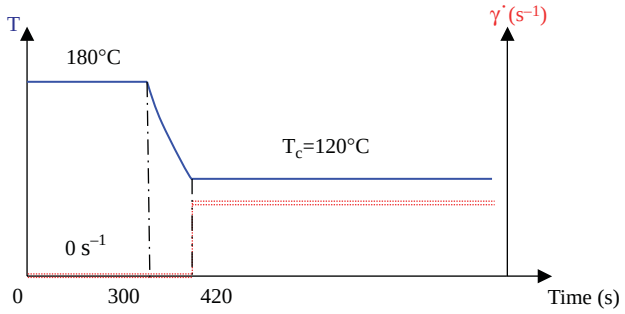

Fig. 1. Thermal path applied to the sample. The rheo-optical measurements start at 420 s.

In the present study the shear rate at the observation point was varied between 0.01 and 0.36 s^{-1}. Due to the high viscosity of the polymer, we were not able to increase further the shear rate.

The rheological experiments were undertaken using a rheometrics dynamic analyser (RDA) equipped with a parallel plate fixture.

The samples were subjected to the following thermal path (Fig. 1). First, the polymer was heated to 180 °C and hold at this temperature during 5 min in order to erase any residual injection-induced crystallization. The sample was then rapidly quenched (30 °C/min) to the testing temperature (120 °C). In order to avoid thermal crystallization effects and its contribution to the optical measurements, the testing temperature, for which the quiescent crystallization kinetics is small, was held constant during the rheo-optical experiments. It is worth to mention at this point that there is another common type of thermo-mechanical conditions reported in the literature [13,14], in which the influence of pre-straining of the polymer melt on the subsequent quiescent crystallization upon cooling is considered. This differs from the present study in which the polymer crystallizes under strain.

Optical measurements were performed using a rheometrics optical train (ROA) [15]. The schematic of the rheo-optical set-up is represented in Fig. 2. It consisted of a linearly polarised He–Ne laser (wavelength of 632.8 nm) followed by a rotary half-wave plate with a rotation frequency of $\omega = 2$ kHz. The polarisation-modulated beam passed then through the flow cell at the observation point. The transmitted beam either passed through a circular polarizer and then collected at a photodiode in birefringence experiments, or directly collected at the photodiode in the case of dichroism measurements. The transmitted intensity of light was finally demodulated using a lock-in amplifier to infer its in-phase and out-of-phase components. The dichroism ($\Delta n''$) and the extinction angle (χ''), or birefringence ($\Delta n'$) and its corresponding extinction angle (χ') could be obtained from the transmitted intensity using the usual Muller calculus method [16]. For the dichroism, we have:

$$\frac{I_2}{I_0^2/2} = 1 - \sinh\delta''\cos 2\chi''\cos 4\omega t - \sinh\delta''\sin 2\chi''\sin 4\omega t$$

The magnitude of the dichroism is then inferred from the following relationship:

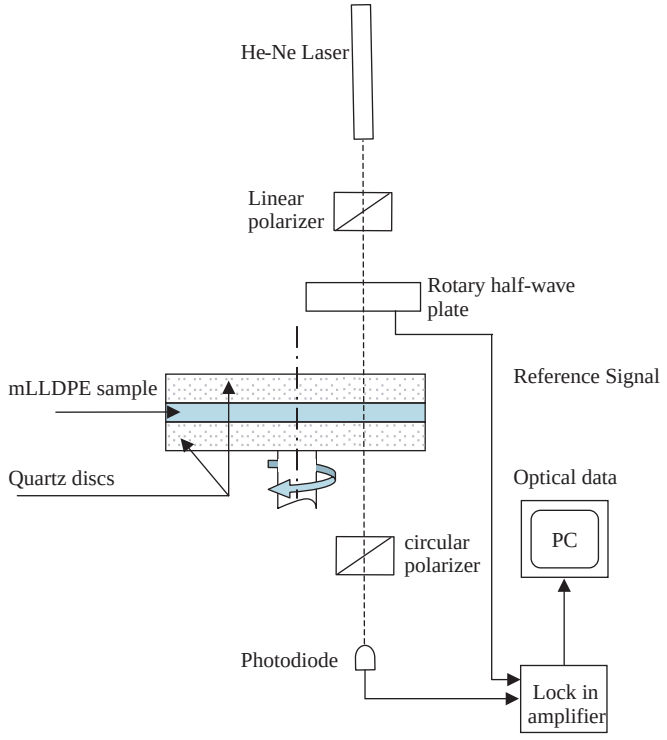

Fig. 2. Rheo-optical set up used for the optical measurements.

$$\delta'' = \frac{2\pi d \Delta n''}{\lambda}$$

(λ is the wave-length and d the optical path).

Similarly, the birefringence properties can be obtained from the transmitted intensity components using the following relationship [16]:

$$\frac{I_1}{I_0^1/4} = 1 + [-\sinh \delta'' \cos 2\chi'' + \sin \delta'' \sin 2\chi'] \cos 4\omega t$$

$$-[\sinh \delta'' \sin 2\chi'' + \sin \delta' \cos 2\chi'] \sin 4\omega t$$

The birefringence can be then obtained using the relationship:

$$\delta' = \frac{2\pi d \Delta n'}{\lambda}.$$

I_0^1 and I_0^2 are the incident intensities, respectively for birefringence and dichroism measurements.

From the above equations, we can note that there is a coupling between the birefringence and dichroism. However, the dichroism was found to be more than an order of magnitude smaller than the birefringence. Its contribution to the birefringence terms could be then neglected.

3. Results and discussions

3.1. Evolution of the turbidity

The first optical indication that the crystallisation process is taking place is the attenuation of the transmitted light, or turbidity. The appearance of turbidity is a result of the presence in the material of microstructures (here crystallites) on the length scale of the wavelength and having a refractive index different from that of the matrix. These objects give rise to light scattering and then turbidity. Fig. 3 represents the time evolution of the transmitted light intensity for different shear rates, including the quiescent crystallization.

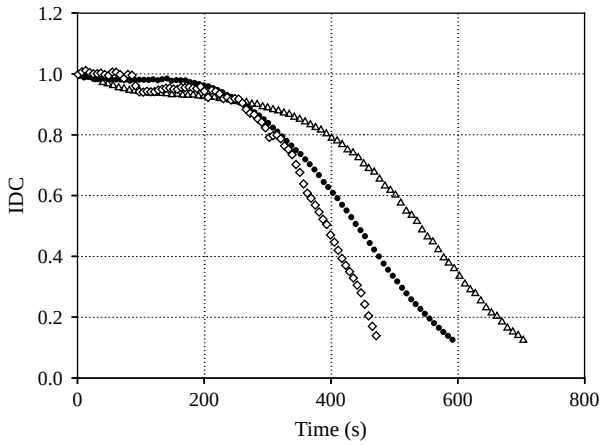

Fig. 3. Evolution of transmitted intensity (normalized to its initial value) versus time for different shear rates. (△) Thermal crystallization ($\dot{\gamma} = 0\ s^{-1}$), (●)$\dot{\gamma} = 0.01\ s^{-1}$, (■)$\dot{\gamma} = 0.1\ s^{-1}$.

In light of the turbidity evolution we can assume that the crystallization process develops through two different stages. First, the transmitted intensity decreases slowly, which would correspond to a nucleation phase, and in a second stage the intensity decreases more rapidly, which would correspond to a growth phase. Such separation of shear-induced crystallization into two regimes is well-known in the literature, in particular through the evolution of the rheological behaviour of polymer [17–19].

In order to quantify the duration of the two aforementioned crystallization stages, we can define two characteristic times: an induction time t_0 and a characteristic time of the crystalline growth τ. We can see in Fig. 3 that the transition between the two stages takes place when the transmitted intensity decreases for about 10%. Then, t_0 can be defined to be the time for which the intensity decrease is 10%. τ can be inferred from the slope of the intensity curve at the point where the transmitted intensity is divided by a factor 2. Fig. 4 represents the evolution of the characteristic time of the crystalline growth and that of the nucleation phase as a function of shear rate. Error bars in Fig. 4 corresponds to the 95% confidence intervals calculated using typically 5 runs. Unexpectedly, our results show that the influence of the shear rate on the induction time is rather small. That is, the nucleation kinetics seems to be almost independent upon shear rate. A possible explanation is that the shear rates involved in our experiments are too low (compared the relaxation rate of the polymer) to lead to such dependence. Indeed, oscillatory shear measurements performed during the induction time led to a terminal relaxation time of 0.03 s, which suggests that one has to shear the polymer at rates higher than $30\ s^{-1}$ to obtain a significant segmental net orientation of the polymer and then a shear-rate dependence of the nucleation growth. On the other hand, the duration of the crystalline growth phase depends more clearly upon the shear rate: As

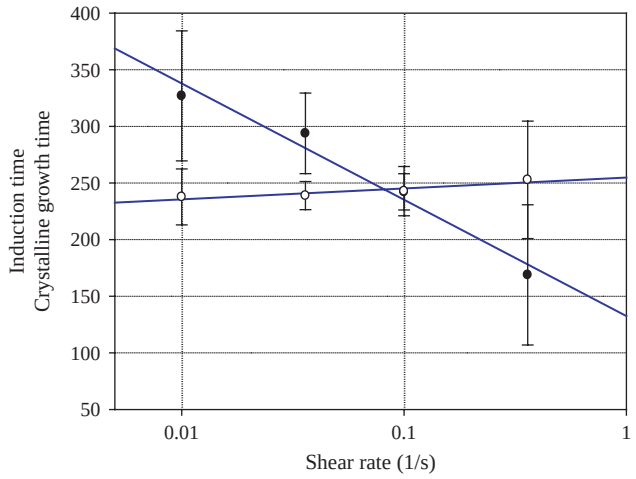

Fig. 4. Induction time and crystalline growth characteristic time versus shear rate.

expected it decreases with shear rate. This can be understood as the following. During the course of the crystallization process the effective viscosity of the polymer increases, leading to the slowing down of the molecular relaxation rate. This can make possible a shear-induced orientation of molecular segments even at relatively small shear rates, leading then to flow-enhancement of the crystallization process.

3.2. Birefringence evolution

The birefringence arises from anisotropic orientation of molecular segments. Then, both the flow-induced segmental orientation in the amorphous phase and the segments belonging to crystallites may contribute to the birefringence. An additional physical measurement sensitive to only one phase (X-ray diffraction [20,21], for instance) would be then useful in order to distinguish between the two contributions to the birefringence.

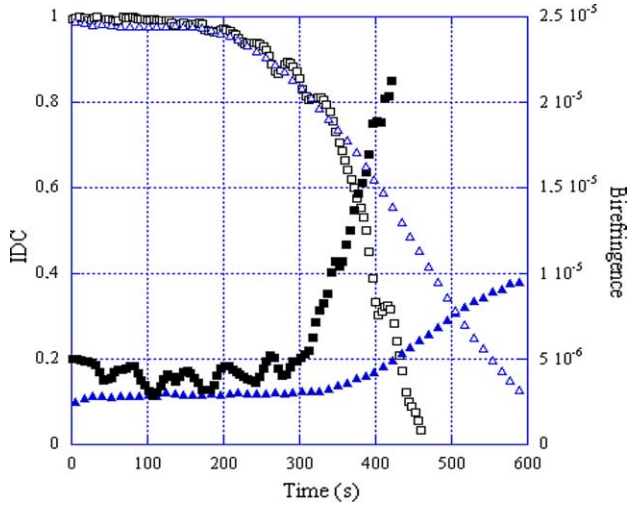

Fig. 5. Evolution of birefringence (filled symbols) and transmitted light intensity (open symbols) versus time for two different shear rates, (▲, △) $\dot{\gamma} = 0.01\ s^{-1}$ and (■, □) $0.36\ s^{-1}$.

The time evolution of the birefringence is compared to that of the turbidity in Fig. 5, for the smallest and the highest shear rates used in our experiments (0.01 and $0.36\ s^{-1}$). Similarly to the turbidity the time evolution of the birefringence can be split into two stages. At a first stage the birefringence remains approximately constant and comparable with that obtained for the polymer in the molten state (at 180 °C). In a second stage, the birefringence significantly increases at a rate depending upon the shear rate. The birefringence remains positive, indicating a net segmental orientation in the flow direction, since the polymer has a positive stress-optical coefficient. Even though the increase of the birefringence is correlated with the decrease of the transmitted intensity (Fig. 5), we observe some delay between the starting points of the evolution of these two optical properties. For both shear rates represented in Fig. 5, the transmitted light starts to decrease after about 200 s of shearing, while the birefringence starts to significantly increase only after 300 s. This delay can be explained as the following. Due to molecular relaxation, the shear rates involved here are too small to lead to a net orientation of chain segments and to give a measurable birefringence before onset of crystallisation or when the crystallization level is too low (first stage). As the crystalline phase volume fraction increases, the relaxation of the chain segments slows down giving rise to an average segmental orientation in the flow direction, and in turn an increase of the birefringence (second stage). Between 200 and 300 s, although the turbidity indicates that the crystallization process is taking place, the molecular relaxation rate may be still too high compared to the shear rate to lead to a net segmental orientation.

In Fig. 6 we represent the evolution of birefringence versus time (strain) for different shear rates, including the quiescent state. As expected, quiescent crystallization does not lead to any preferential segmental orientation, in contrast to the results of Floudas et al. [7]. The birefringence measurements were

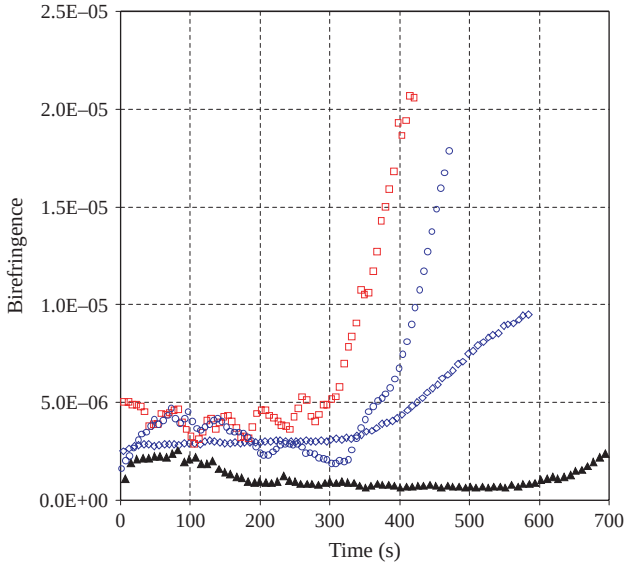

Fig. 6. Evolution of birefringence versus time for different shear rates. (▲) quiescent crystallization ($\dot{\gamma} = 0\ s^{-1}$), (■) $\dot{\gamma} = 0.01\ s^{-1}$, (○) $\dot{\gamma} = 0.1\ s^{-1}$, (□) $\dot{\gamma} = 0.36\ s^{-1}$.

assumed to be meaningless when the transmitted intensity was too small. We stopped birefringence measurements for the same minimum transmitted intensity for all the experimental runs. If we assume that the crystalline volume fraction is the same for the same turbidity, the birefringence results (Fig. 6) show that the final level of the semi-crystalline anisotropy increases with the shear rate.

Floudas et al. [7] reported similar experiments in the case of poly(ε-caprolactone). Their results are qualitatively different from ours. Indeed, they observed a bell-shape behaviour of both birefringence and dichroism. This was explained by assuming that the crystalline growth was first anisotropic, and became isotropic at the end stage of crystallization. We do not observe such maxima in the case of our experiments. A possible explanation is the following. In Floudas et al. [7] experiments the shearing is performed at a controlled stress. Then the shear rate will decrease with strain since the crystallization leads to the increase of the effective viscosity of the polymer. The decrease of the shear rate would lead to the decrease of the birefringence and dichroism. In contrast, in our experiments the shear rate is fixed. This would be the reason why we do not observe a bell-like behaviour of neither the birefringence nor the dichroism as it will be seen below.

3.3. Dichroism evolution and comparison with birefringence

The dichroism corresponds to anisotropic scattering of light, which results in a polarisation-dependent attenuation of light. This happens when anisotropic crystallites with a size on the order of the light wavelength appear in the system. Fig. 7 represents the time evolution of the dichroism compared to that of the turbidity in the case of the smallest and the highest shear rates involved in our experiments. Similarly to the birefringence, we have a significant increase of dichroism only after some advance in the crystallization process.

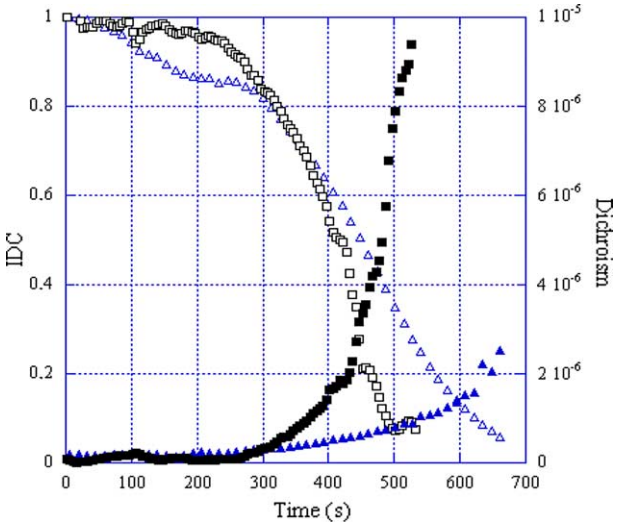

Fig. 7. Evolution of dichroism (filled symbols) and transmitted light intensity (open symbols) versus time for two different shear rates, (▲, △) $\dot{\gamma} = 0.01\ s^{-1}$ and (■, □) $0.36\ s^{-1}$.

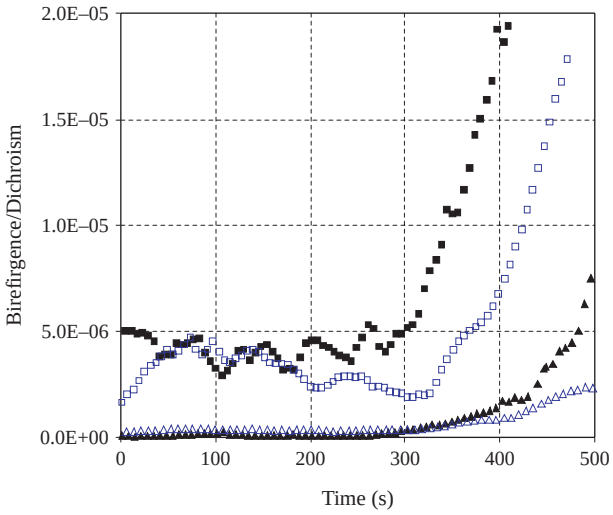

Fig. 8. Evolution of birefringence (■) and dichroism (▲) for two different shear rates: (■, ▲): $\dot{\gamma} = 0.36\ s^{-1}$; (□, △): $0.01\ s^{-1}$.

Birefringence and dichroism evolutions with time are compared to each other in Fig. 8 for two different shear rates. As it is generally the case, the birefringence is more than an order of magnitude higher than the dichroism. One of the possible reasons is that only the crystallites would contribute to the dichroism, while both crystalline and amorphous phases may contribute to the birefringence. It is to be noted that the oscillations of birefringence we observe in Fig. 8 may not have any physical origin, but may be rather due to an experimental artefact. It is hard to say if there is any delay between birefringence and dichroism on the basis of the representation in Fig. 8.

3.4. Stress evolution and comparison with the optical properties

The crystallization development of a polymer has often been followed through the evolution of its rheological properties. Taking advantage of the similarity between crystallization, in particular at its early stage, and physical gelation, it is possible to follow the crystallization process by monitoring the polymer's linear viscoelastic properties [22–24]. However, this method can be only used in the case of quiescent crystallization. In the case of a polymer crystallizing under strain the crystallization development can be followed mechanically through the evolution of the effective viscosity (or stress) [25]. The crystallites will act as reinforcement in a nanocomposite material giving rise to a huge increase of the stress. The question is at what extent can we infer information about the semi-crystalline microstructure through the analysis of the stress evolution.

The time evolution of the polymer's effective viscosity at different fixed shear rates is represented in Fig. 9. The rheological experiments were performed under the same thermo-mechanical conditions, including the thermal path and the flow geometry, than those of the optical ones. As expected, after a certain induction time, which as usual represents the major part of the duration of the crystallization

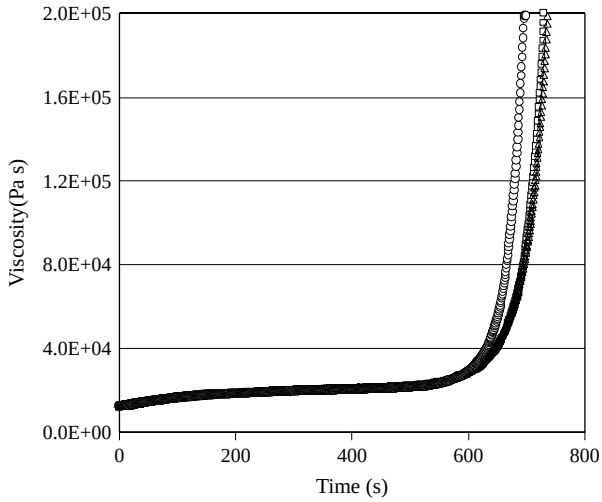

Fig. 9. Time evolution of the effective viscosity for different shear. rates: 0.01 s^{-1} (○); 0.1 s^{-1} (□); 0.36 s^{-1} (△).

process, we observe a huge increase of the effective viscosity. The shear rate dependence of the crystallization development is much less pronounced in the stress behaviour than in the optical ones. Moreover, we observe a significant delay (about 200 s) between the onset of the optical properties variation and that of stress rise. The origin of this delay may be attributed to at least the two following reasons:

(i) In parallel plates flow geometry, the polymer is subjected to a non-homogeneous shear rate. The polymer may then start to crystallize at the edge of the plates where the shear rate is the highest. Near the plate's axis, where the shear rate is zero, the polymer would crystallize in almost a quiescent state. The measured stress is an average value of the viscous forces exerting on the whole surface of the plate, while the measured optical properties are local values even though in both cases, an average is undertaken over the sample thickness. However, the material would be nearly homogeneous over the thickness if we can ignore boundary effects. Consequently, the optical and the mechanical properties are not related to the same state of the material and would not vary accordingly.

(ii) With the optical technique used here, which is based on a polarization–modulation technique, we can detect very low level (up to 10^{-9} in polarimetry) of induced anisotropy in the material. The mechanical measurements are much less accurate. Moreover, it has been showed experimentally [11] that at the early stages of a strain-induced crystallization the stress-optical coefficient is higher than that of the corresponding amorphous polymer. The stress-optical coefficient C is defined through the relationship $\Delta n' = C\sigma$, where σ is the stress. This would increase further the sensitivity of polarimetry measurements compared to that of the mechanical ones in the early stages of the crystallization process.

Fig. 10 represents the evolution of the effective viscosity as a function of shear rate at three different times. At 150 s,

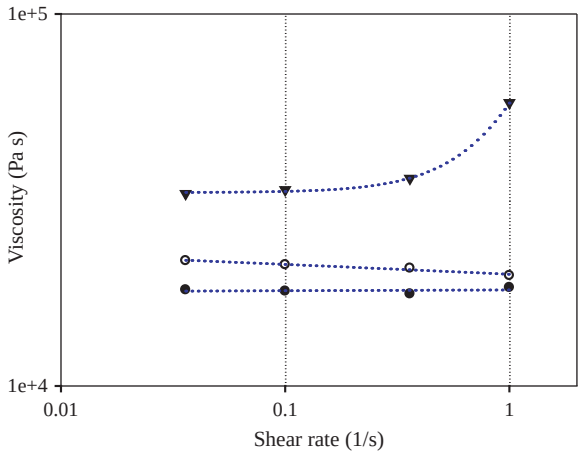

Fig. 10. Rheogram of the semi-crystalline polymer at different instants of the crystallization process: 150 s (●); 450 s (○); 620 s (▼).

according the optical properties the polymer may be still amorphous in the shear rate interval investigated. The fact that the polymer is Newtonian suggests that we have no strain induced orientation (in the flow direction) in this case. As discussed above this may be attributed to the fact the shear rates involved here are too small compared to the relaxation rate of the polymer chains.

$t = 450$ s corresponds to the moment where the optical properties are significantly evolving. In this case, we obtain a slight decrease of the viscosity as a function of shear rate. This net shear-thinning aspect is rather small ($\mu = A\dot{\gamma}^{1-n}$, $n = 0.973$). However, the rheogram for $t = 450$ is a combination of two opposing effects: the shear-thinning contribution of the amorphous phase and the shear-thickening aspect due the increase of the crystallinity ratio as a function of shear rate. The shear-thinning contribution of the amorphous phase due to segmental orientation would be then more significant than can be inferred from the rheogram. This suggests that there may be some strain-induced orientation in the amorphous phase, which would contribute then to the birefringence.

At high level of crystallisation ($t = 620$ s) the shear-thickening effect due the increase of crystalline ratio as a function of shear rate is dominant.

4. Conclusion

We have presented in this paper on-line measurements of the optical properties of an mLLDPE sample undergoing crystallization under shear flow. Through the three optical properties investigated, including the turbidity, birefringence and dichroism, it was possible to characterize the semi-crystalline microstructure evolution in the material. Three different stages of the crystallization process, including a nucleation phase, an isotropic crystallite growth and finally an anisotropic growth stage, could be distinguished. These different stages were suggested by the presence of delays between the moments where the three different optical properties investigated started to significantly evolve.

The optical properties evolution due the development of the crystallization was compared to that of the stress under the

same thermo-mechanical conditions. It was observed that the optical properties were more sensitive than the stress to follow the crystalline development, in particular during the early stages of the process. This was attributed to the fact that the optical measurements were highly accurate and local, while the measured stress was an average value over a domain in which the material was highly heterogeneous.

References

[1] Verboten O. PhD Thesis, Université Catholique de Louvain; 1997.
[2] Vigny M, Tassin JF, Giraud A, Lorentz G. Polym Eng Sci 1997;37(11): 1785.
[3] Salem DR. Polymer 1992;33:3182.
[4] Vigny M, Tassin JF, Lorentz G. Polymer 1999;42(2):397.
[5] Blundell DJ, Mahendrasingam A, Martin C, Fuller W, MacKerron DH, Harvie JL, et al. Polymer 2000;41:7793.
[6] Chaari F, Chaouche M, Doucet J. Polymer 2003;44(2):473.
[7] Floudas G, Hilliou L, Lellinger D, Alig I. Macromolecules 2000;33:6466.
[8] Bushman AC, McHugh AJ. J Appl Polym Sci 1997;64(11):2165.
[9] Swartjes FHM, Peters GWM, Rastogi S, Meijer HEH. Int Polym Proc 2003;18(1):53.
[10] Janeschitz-Kriegl H, Wippel H, Lin JP, Lipp M. Rheol Acta 2001;40(3): 248.
[11] Ryu DS, Inoue T, Osaki K. Polymer 1998;39(12):2515.
[12] Yan RJ, Ajji A, Shinozaki DM, Dumoulin MM. Polymer 2000;41(3): 1077.
[13] Chai CK, Azoux Q, Randrianatoandro H, Navard P, Haudin JM. Polymer 2003;44(3):773.
[14] Kumaraswamy G, Issaian AM, Kornfield JA. Macromolecules 1999; 32(22):7537.
[15] Le Meins J-F, Tassin J-F, Corpat JM. J Rheol 1999;43(6):1423.
[16] Fuller GG. Optical rheometry of complex fluids. New York: Oxford University; 1995.
[17] Yoon WJ, Myung HS, Kim BC, Im SS. Polymer 2000;41(13):4933.
[18] Gorlier E, Haudin JM, Billon N. Polymer 2001;42:9541.
[19] Madbouly SA, Ougizawa T. J Macromol Sci Phys 2003;B42(2):269.
[20] Kumaraswamy G, Kornfield JA, Yeh FJ, Hsiao BS. Macromolecules 2002;35(5):1762.
[21] Wiyatno W, Pople JA, Gast AP, Waymouth RM, Fuller GG. Macromolecules 2002;35(22):8488.
[22] Pogodina NV, Winter HH. Macromolecules 1998;31(23):8164.
[23] Gelfer MY, Horst RH, Winter HH, Heintz AM, Hsu SL. Polymer 2003; 44(8):2363.
[24] Gelfer MY, Winter HH. Macromolecules 1999;32(26):8974.
[25] Eder G, Janeschizt-Kriehl H, Liedauer S. Prog Polym Sci 1989;15:629.